Chapter 2

THE WAVE PROPAGATION METHOD

In this chapter we introduce the concept of a hyperbolic conservation law and develop a numerical solution technique known as the *wave propagation method* for the spatio-temporal dynamics of these equations. In the case of 2D spatial dynamics to which we restrict ourselves in this work, the wave propagation method described in this chapter is numerically conservative, second order accurate for smooth solutions, total variation diminishing for non-smooth solutions, shock capturing, and numerically stable up to a Courant number of one.

2.1 Conservation laws

A quantity q is said to be *conserved* if the amount of q in some region Ω can only be modified in time by the flux of q through the boundary of Ω:

$$\partial_t \int_\Omega q\, dV = \text{net flux across the boundary of } \Omega. \tag{2.1}$$

If we now define a flux function F, we can rewrite (2.1) in the form:

$$\partial_t \int_\Omega q\, dV + \int_{\partial\Omega} F \cdot \mathbf{n}\, dA = 0\,, \tag{2.2}$$

where $\Omega \subset \mathbb{R}^n$ is the domain over which q is conserved, $\partial\Omega$ is the boundary of this domain, $\mathbf{n}$ is the outward pointing unit normal to $\partial\Omega$, dV is a volume element, and dA is a surface area element. Under the assumption of smoothness on q, Gauss' divergence theorem can be applied to (2.2) to obtain

$$\int_{d\Omega} F \cdot \mathbf{n}\, dA = \int_\Omega \nabla \cdot F\, dV\,. \tag{2.3}$$

The smoothness assumption also allows us to pull the time derivative in (2.2) inside the volume integral. Applying these simplifications results in

$$\int_\Omega \Big(\partial_t q + \nabla \cdot F\Big)\, dV = 0\,. \tag{2.4}$$

If the above equation is to be a conservation law, equation (2.4) must be valid for all domains Ω. This implies that the integral conservation law (2.2) under a smoothness assumption on q is equivalent to a partial differential equation of the form

$$\partial_t q + \nabla \cdot F = 0\,. \tag{2.5}$$

In this work, we focus on developing numerical methods that directly solve (2.5), but appeal to the original integral conservation law (2.2) in regions where the q is not smooth.

2.2 Hyperbolic conservation laws and the Riemann problem

Many partial differential equation can be classified as either *elliptic*, *parabolic*, or *hyperbolic*. Associated with each of these types is a canonical equation from classical physics [45]. The classical hyperbolic equation is the *wave equation*:

$$\partial_t^2 \phi - \partial_x^2 \phi = 0 \tag{2.6}$$
$$\phi(x, 0) = g(x) \,. \tag{2.7}$$

This equation has the property that initial condition $g(x)$ will be partitioned into two distinct pieces: (a) a left-going piece that propagates with a velocity equal to -1 and (b) a right-going piece that propagates with a velocity equal to 1. Unlike elliptic and parabolic equations, information for the hyperbolic equation travels at finite speeds [45]. Waves propagating at a finite speed occur in many important physical applications; and therefore, it is important to develop numerical methods for solving the wave equation and its generalizations. The remainder of this chapter is devoted developing a numerical method for solving hyperbolic partial differential equations that can be written as conservation laws.

2.2.1 Hyperbolic conservation laws

In this section, we make rigorous what hyperbolicity means for a conservation law (2.5). We begin by defining the *flux Jacobian*:

$$A^\star \equiv \frac{\partial}{\partial q} \left(F \cdot \omega \right) , \tag{2.8}$$

where $|\omega| = 1$ is a vector that picks out a specific direction from the flux function. The dimensions of the variables in (2.8) are as follows:

$$q \in \mathbb{R}^m, \;\; F \in \mathbb{R}^{m\times n}, \;\; \omega \in \mathbb{R}^n, \;\; \text{and} \;\; A^\star \in \mathbb{R}^{m\times m} \,,$$

where m is the number of unknowns and n is the number of space dimensions.

Definition 2.2.1 *Equation (2.5) is* **hyperbolic** *if, for any $q \in \Omega$ and for any $\omega \in \mathbb{R}^n$ such that $|\omega| = 1$, the matrix $A^\star$ has m real eigenvalues with a complete family of right eigenvectors. Furthermore, the system is said to be* **strictly hyperbolic** *at a state q if the eigenvalues at this state are also distinct (definition taken from [34]).*

As will be seen in subsequent sections, the eigenvalues of the flux Jacobian are directly related to the *wave speeds* of solutions to the conservation law. Since the eigenvalues are required to be real, dynamics governed by hyperbolic conservation laws necessarily involve information propagating at finite speeds. In the example below, we show how the wave equation can be recast as a hyperbolic conservation law.

Example 2.2.2 *The wave equation (2.6) can be written as a system of two scalar equations if the variables* p *and* u *are defined such that*

$$p \equiv -\partial_t \phi \tag{2.9}$$
$$u \equiv \partial_x \phi \,. \tag{2.10}$$

Plugging these definitions into (2.6) and requiring that $\partial_{xt}\phi = \partial_{tx}\phi$ *for consistency yields the following conservation law:*

$$\partial_t \begin{bmatrix} p \\ u \end{bmatrix} + \partial_x \begin{bmatrix} u \\ p \end{bmatrix} = 0 \,. \tag{2.11}$$

The flux Jacobian is given by

$$A = \begin{bmatrix} 0 & 1 \\ 1 & 0 \end{bmatrix} \tag{2.12}$$

for which the eigenvalues are $\lambda = \pm 1$*. Therefore, the wave equation written in the form (2.11) is a strictly hyperbolic conservation law.*

2.2.2 The 1D Riemann problem

To further explore the wave solutions to hyperbolic conservation laws, we consider a special initial value problem for the one dimensional equation

$$\partial_t q + \partial_x f(q, x) = 0 \tag{2.13}$$

called the *Riemann problem.* The initial condition for the Riemann problem is a piecewise constant profile that is discontinuous at the point $x = x_0$:

$$q(x,0) = \begin{cases} Q_l & \text{if } x < x_0 \\ Q_r & \text{if } x > x_0 \,. \end{cases} \tag{2.14}$$

In the case where the flux function f depends explicitly on x, we require that this spatial dependence is of the form

$$f(q,x) = \begin{cases} f_l(q) & \text{if } x < x_0 \\ f_r(q) & \text{if } x > x_0 \,. \end{cases} \tag{2.15}$$

In general, these initial conditions are not a steady state solution to conservation law (2.13); and therefore, we expect the solution to the Riemann problem to be an *adjustment* process to some final steady state. Furthermore, since (2.13) is assumed to be hyperbolic, we expect this adjustment process to involve waves propagating at finite speeds.

2.2.3 The Riemann problem for constant coefficient linear equations

The constant coefficient linear version of (2.13) takes the form

$$\partial_t q + A\,\partial_x q = 0 \tag{2.16}$$
$$q(x,0) = \begin{cases} Q_l & \text{if } x < x_0 \\ Q_r & \text{if } x > x_0 \,. \end{cases} \tag{2.17}$$

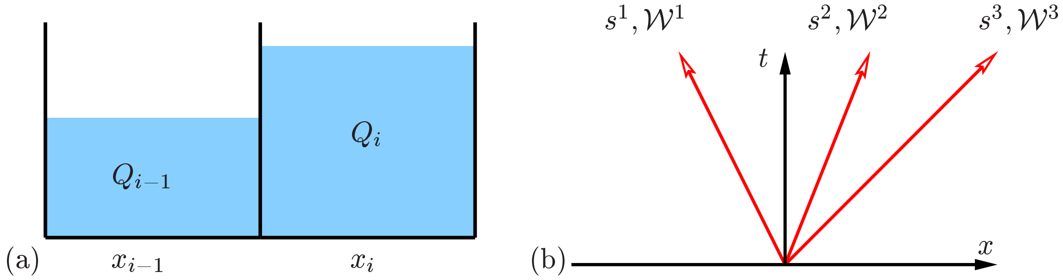

Figure 2.1: The Riemann problem (a) after piecewise constant averaging and (b) after adjustment through the generation of waves propagating at finite speeds.

Under the hyperbolicity assumption the flux Jacobian can be written as

$$A = R\Lambda R^{-1}\,, \tag{2.18}$$

where Λ is the diagonal matrix of eigenvalues, R is the matrix of right eigenvectors, and R^{-1} is the matrix of left eigenvectors. These matrices can be written as follows:

$$R = \left[r^1 \middle| \cdots \middle| r^m \right], \ \Lambda = \text{diag}\left(\lambda^1, \cdots, \lambda^m\right), \ R^{-1} = \left[l^1 \middle| \cdots \middle| l^m \right]^t, \tag{2.19}$$

where r^ℓ and l^ℓ are of dimension $m \times 1$ and denote the ℓ^{th} right and left eigenvectors, respectively. The right and left eigenvectors are orthonormal to each other and satisfy

$$r^i \cdot l^j = \begin{cases} 1 & \text{if } i = j \\ 0 & \text{if } i \neq j\,. \end{cases} \tag{2.20}$$

Using the above information, (2.16) can be rewritten as follows:

$$\partial_t q + A\,\partial_x q = 0 \tag{2.21}$$

$$\implies \quad \partial_t q + R\Lambda R^{-1}\partial_x q = 0 \tag{2.22}$$

$$\implies \quad R^{-1}\partial_t q + \Lambda R^{-1}\partial_x q = 0 \tag{2.23}$$

$$\implies \quad \partial_t\left(R^{-1}q\right) + \Lambda\,\partial_x\left(R^{-1}q\right) = 0 \tag{2.24}$$

$$\implies \quad \partial_t\left(l^p q\right) + \lambda^p\,\partial_x\left(l^p q\right) = 0\,. \tag{2.25}$$

In equation (2.25), the variable $l^p q$ is completely decoupled from all the other components of $R^{-1}q$. Therefore, (2.25) is a simple advection equation for the scalar unknown $l^p q$ and its solution is given by

$$l^p q(x,t) = l^p q(x - \lambda^p t, 0)\,, \tag{2.26}$$

where $q(x,0)$ is the initial condition [45]. The full solution $q(x,t)$ can now be obtained from the superposition of all m advection equation solutions:

$$q(x,t) = \sum_{p=1}^{m} l^p q(x - \lambda^p t, 0)\, r^p\,. \tag{2.27}$$

Plugging in the initial condition (2.17), we see that the solution to the Riemann problem is a decomposition of the initial jump into a set of m smaller discontinuities that occur along the m eigenvectors (r^p) and that travel at speeds that are equal to the corresponding eigenvalue (λ^p). This is referred to as a *wave decomposition* and is illustrated in Figure 2.1. Mathematically, the wave decomposition process can be written as

$$\Delta Q \equiv Q_r - Q_l = \sum_{p=1}^{m} (l^p \Delta Q)\, r^p \equiv \sum_{p=1}^{m} \alpha^p r^p \equiv \sum_{p=1}^{m} \mathcal{W}^p\,, \tag{2.28}$$

where $\mathcal{W}^p$ is referred to as the p^{th} *wave*.

We stated earlier that the differential equation formulation of a conservation law is only valid for smooth solutions. It can be shown, however, that the discontinuous solutions derived thus far are completely consistent with the integral formulation [53]. On the other hand, there are certain results which can only be obtained by looking directly at the integral conservation law. One such result is the *Rankine-Hugoniot condition*. This condition is derived in [53] and states that the jump in flux ($\mathcal{Z}$) and the jump in q ($\mathcal{W}$) across a discontinuity propagating at speed s are related by the formula

$$\mathcal{Z} = s\mathcal{W}\,. \tag{2.29}$$

Such a discontinuity is often referred to as a *shock* or *shock wave*. Therefore, the Rankine-Hugoniot conditions tell us that a completely equivalent procedure to (2.28) for solving the constant coefficient Riemann problem for (2.16) is to decompose the initial flux difference:

$$\Delta f \equiv AQ_r - AQ_l = \sum_{p=1}^{m} (l^p \cdot \Delta f)\, r^p \equiv \sum_{p=1}^{m} \beta^p r^p \equiv \sum_{p=1}^{m} \mathcal{Z}^p\,, \tag{2.30}$$

where $\mathcal{Z}^p$ is the jump in flux across the p^{th} wave and $\mathcal{Z}^p = s^p\mathcal{W}^p$ by the Rankine-Hugoniot conditions. This approach turns out to be advantageous over (2.28) for variable coefficient and nonlinear equations.

2.2.4 The Riemann problem for variable coefficient linear equations

In this section we consider a linear conservation law in which the coefficient matrix is an explicit function of the spatial coordinate. The Riemann problem is given by

$$\partial_t q + \partial_x \left(A(x) q\right) = 0 \tag{2.31}$$

$$q(x,0) = \begin{cases} Q_l & \text{if } x < x_0 \\ Q_r & \text{if } x > x_0 \end{cases} \tag{2.32}$$

$$A(x) = \begin{cases} A_l & \text{if } x < x_0 \\ A_r & \text{if } x > x_0\,. \end{cases} \tag{2.33}$$

We assume that the number of positive and negative eigenvalues of $A(x)$ is identical to the left and right of $x = x_0$. In this case, we define a flux Jacobian at $x = x_0$ such that

$$\bar{A} \equiv R\Lambda R^{-1}\,, \tag{2.34}$$

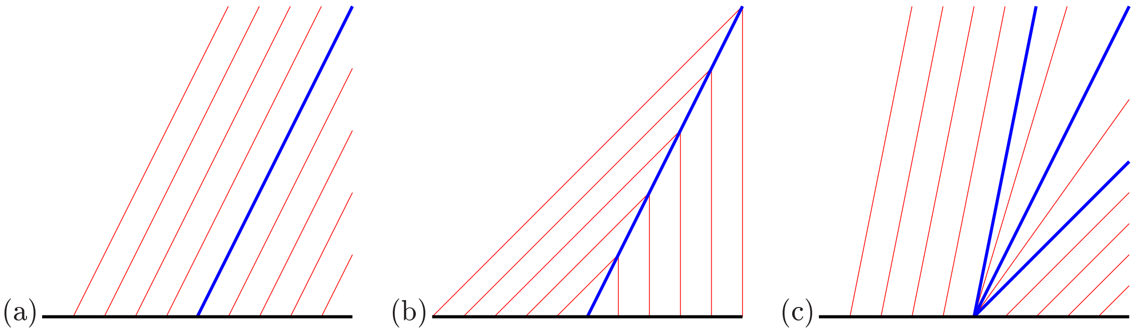

Figure 2.2: Plots of the characteristics in the $x - t$ plane showing examples of (a) a linearly degenerate wave, (b) a nonlinear shock wave, and (c) a nonlinear rarefaction wave.

where the eigenvalue and eigenvector are taken from A_l if the eigenvalue is negative and from A_r if the eigenvalue is positive:

$$R = \left[r_l^1 \middle| \cdots \middle| r_l^k \middle| r_r^{k+1} \middle| \cdots \middle| r_r^m \right] \tag{2.35}$$

$$\Lambda = \operatorname{diag}\left(\lambda_l^1, \cdots, \lambda_l^k, \lambda_r^{k+1}, \cdots, \lambda_r^m \right). \tag{2.36}$$

The Rankine-Hugoniot conditions tell us that after the waves have propagated away from the interface $x = x_0$, the state immediately to the left (Q^-) of $x = x_0$ and the state immediately to the right (Q^+) must satisfy the relationship

$$A_r Q^+ - A_l Q^- = 0\,. \tag{2.37}$$

Therefore, not only does the solution jump across the m waves predicted by $\bar{A}$, but it also jumps across the interface $x = x_0$. This implies that we cannot simply divide the jump $\Delta Q = Q_r - Q_l$ among the m eigenvectors of $\bar{A}$ as was done in the constant coefficient case. On the other hand, the Rankine-Hugoniot conditions tell us that the flux should remain continuous across $x = x_0$ and can only jump across the m eigenvectors of $\bar{A}$.

Combining these two facts tells us that the Riemann problem for (2.31) can be replaced by a Riemann problem for

$$\partial_t q + \bar{A}\partial_x q = 0\,, \tag{2.38}$$

as long as the quantity that is being decomposed across each wave is the flux difference,

$$\Delta f \equiv A_r Q_r - A_l Q_l\,. \tag{2.39}$$

Further discussion of Riemann solvers that are based on flux differences can be found in LeVeque and Pelanti [58] and in Bale et al. [5].

2.2.5 The Riemann problem for nonlinear equations

Finally, we consider the Riemann problem for a nonlinear conservation law:

$$\partial_t q + \partial_x f(q, x) = 0 \tag{2.40}$$

$$q(x, 0) = \begin{cases} Q_l & \text{if } x < x_0 \\ Q_r & \text{if } x > x_0 \end{cases} \tag{2.41}$$

$$f(q, x) = \begin{cases} f_l(q) & \text{if } x < x_0 \\ f_r(q) & \text{if } x > x_0 \,. \end{cases} \tag{2.42}$$

Since we already know how to solve linear Riemann problems, we will try to approximate (2.40) through a linearization at the point $x = x_0$. In particular, we will linearize by constructing an approximate flux Jacobian at the interface $x = x_0$:

$$\bar{A}(Q_l, x_l, Q_r, x_r) \equiv \frac{\partial \bar{f}}{\partial q}\left(\bar{Q}\right) \,, \tag{2.43}$$

where $\bar{Q}$ is some average of Q_l and Q_r and $\bar{f}(q)$ is some average of $f_l(q)$ and $f_r(q)$. This reduces our Riemann problem to one which we already know how to solve:

$$\partial_t q + \bar{A}\partial_x q = 0 \tag{2.44}$$

$$\Delta f \equiv f_r(Q_r) - f_l(Q_l) \,. \tag{2.45}$$

Having applied this simplification, we are faced with the following two questions:

1. How should we chose $\bar{Q}$ and $\bar{f}$ to define the approximate flux Jacobian $\bar{A}$?
2. How accurately do the linear wave solutions represent the nonlinear wave solutions?

Although we will answer Question 1 more rigorously in Section 2.4.2, let us present some common approaches for computing $\bar{Q}$ and $\bar{f}$. The approach presented in [5] for $\bar{f}$ is *arithmetic averaging*:

$$\bar{f}(q) = \frac{1}{2}\Big(f_r(q) + f_l(q)\Big) \,. \tag{2.46}$$

Because it is easy to compute, the first approach we present for computing $\bar{Q}$ is also based on the arithmetic average:

$$\bar{Q} = \frac{1}{2}\left(Q_l + Q_r\right) \,. \tag{2.47}$$

The second approach is referred to as *Roe averaging* and we take the $\bar{Q}$ that makes the following statement true:

$$\frac{\partial \bar{f}}{\partial q}\left(\bar{Q}\right) \cdot \left(Q_r - Q_l\right) = f_r(Q_r) - f_l(Q_l) \,. \tag{2.48}$$

This approach was first introduced by Roe [74] for the Euler equations. For an example see Section 4.2.3 in which the Roe averages for the shallow water magnetohydrodynamic equations are computed. The Roe average is very useful because if the exact solution to the nonlinear Riemann is a single wave carrying the entire jump in Q, the Roe linearized solution will exactly reproduce this solution [53]. The problem with the Roe average is that it may be too difficult to compute for some conservation laws. In that situation, the natural choice is the arithmetic average.

Finally, we must concern ourselves with Question 2 regarding the accuracy of the linearized Riemann solution as compared with the Riemann solution of (2.40). In general, the solution to a nonlinear Riemann problem consists of more complicated waves than the traveling discontinuities found for linear problems. In particular, each wave can be classified as either linear or nonlinear:

$$p^{\text{th}} \text{ wave} = \begin{cases} \text{linear} & \text{if } \nabla\lambda^p \cdot r^p = 0 \\ \text{nonlinear} & \text{if } \nabla\lambda^p \cdot r^p \neq 0\,. \end{cases} \tag{2.49}$$

A linear wave has the same features as those waves found in a linear Riemann solution and a nonlinear wave can either be a *compressional/shock* wave or a *rarefaction* wave (see [53]):

$$p^{\text{th}} \text{ wave} = \begin{cases} \text{linear wave} & \text{if characteristics are } \textbf{parallel} \\ \text{shock wave} & \text{if characteristics are } \textbf{converging} \\ \text{rarefaction wave} & \text{if characteristics are } \textbf{diverging}\,. \end{cases} \tag{2.50}$$

The difference between these three waves is illustrated in Figure 2.2. The linearized Riemann solution will accurately approximate linear waves and shock waves since they appear as traveling discontinuities. The representation of a rarefaction wave will be less accurate, since this continuously varying wave will also be represented by a single jump discontinuity. In practice, however, it turns out that this error is entirely acceptable in almost all circumstances except for one: *a transonic rarefaction*. A transonic rarefaction occurs when the rarefaction is part left-going and part right-going with respect to the reference frame fixed at $x = x_0$. In this case, the linearized Riemann solution will consist of a *single* jump discontinuity which is either left *or* right traveling instead of the rarefaction wave which is both left *and* right traveling. This failure to send information in both coordinate directions can result in an entropy violating weak solution. In such a situation, we will have to modify our linearized Riemann solver by introducing an entropy fix [53]. We present such an entropy fix in Section 2.4.3.

2.3 Finite volume methods and numerical conservation

In this work, we restrict ourselves to considering only hyperbolic conservation laws in two space dimensions. Under this assumption, equation (2.5) can be written in Cartesian coordinates as

$$\partial_t q + \partial_x f_1(q,x,y) + \partial_y f_2(q,x,y) = 0\,, \tag{2.51}$$

where $f_1(q,x,y)$ and $f_2(q,x,y)$ are the fluxes in the x- and y-directions, respectively. We seek a consistent numerical discretization of the above equation that makes use of the fact that $q(x,y,t)$ is a conserved quantity. We begin by considering the rectangular domain

$\Omega \in [x_a, x_b] \times [y_a, y_b]$ and discretize it in the following way:

$$x_i \equiv x_a + (i - 0.5)\left(\frac{x_b - x_a}{m_x}\right) = x_a + (i - 0.5)\Delta x \tag{2.52}$$

$$y_j \equiv y_a + (j - 0.5)\left(\frac{y_b - y_a}{m_y}\right) = y_a + (j - 0.5)\Delta y \tag{2.53}$$

$$t_n \equiv t_0 + n\Delta t\,, \tag{2.54}$$

where m_x and m_y are the number of points in the x- and y-directions and Δx, Δy, and Δt are the step sizes in the x, y, and t variables, respectively. Having made these definitions, we focus on a single *grid cell* centered at (x_i, y_j) and bounded by the rectangle $\mathcal{C}_{ij} \equiv [x_{i-1/2}, x_{i+1/2}] \times [y_{j-1/2}, y_{j+1/2}]$. An approximation to the average amount of q at time $t = t_n$ in this grid cell is denoted by

$$Q_{ij}^n \approx \frac{1}{\Delta x \Delta y} \int_{y_{j-1/2}}^{y_{j+1/2}} \int_{x_{i-1/2}}^{x_{i+1/2}} q(\xi, \eta, t_n)\, d\xi\, d\eta\,. \tag{2.55}$$

As is shown in Figure 2.3, the above grid cell averaging produces a piecewise constant representation of the solution $q(x, y, t)$ in Ω. The time averaged flux of q from $t = t_n$ to $t = t_{n+1}$ across the cell interface located at $x_{i-1/2}$ and the cell interface located at $y_{j-1/2}$ can be written as

$$[\mathcal{F}_1]_{i-1/2,j}^{n+1/2} \approx \frac{1}{\Delta t} \int_{t_n}^{t_{n+1}} f_1\big(q(x_{i-1/2}, y_j, \tau), x_{i-1/2}, y_j\big)\, d\tau \tag{2.56}$$

$$[\mathcal{F}_2]_{i,j-1/2}^{n+1/2} \approx \frac{1}{\Delta t} \int_{t_n}^{t_{n+1}} f_2\big(q(x_i, y_{j-1/2}, \tau), x_i, y_{j-1/2}\big)\, d\tau\,, \tag{2.57}$$

respectively. Conservation now tells us that Q_{ij}^{n+1} must be equal to Q_{ij}^n minus the flux of q out of the bounding rectangle $\mathcal{C}_{ij}$:

$$Q_{ij}^{n+1} = Q_{ij}^n - \frac{\Delta t}{\Delta x}\left([\mathcal{F}_1]_{i+1/2,j}^{n+1/2} - [\mathcal{F}_1]_{i-1/2,j}^{n+1/2}\right) - \frac{\Delta t}{\Delta x}\left([\mathcal{F}_2]_{i,j+1/2}^{n+1/2} - [\mathcal{F}_2]_{i,j-1/2}^{n+1/2}\right)\,. \tag{2.58}$$

Update (2.58) represents the general update for a Cartesian finite volume method. Many different types of finite volume method can be constructed by taking different approximations to the numerical fluxes. Some examples include the well-known Lax-Friedrichs, Lax-Wendroff, Godunov, Beam-Warming, and Fromm's methods [53]. Independent of how these fluxes are computed, however, update (2.58) guarantees *numerical conservation.* This last statement can be verified by defining a quantity M^n which we refer to as the *total mass* in the computational domain Ω:

$$M^n \equiv \Delta x \Delta y \sum_{i=1}^{m_x} \sum_{j=1}^{m_y} Q_{ij}^n \approx \int_{x_a}^{x_b} \int_{y_a}^{y_b} q(\xi, \eta, t)\, d\xi\, d\eta\,. \tag{2.59}$$

In direct analogy to conservation in the continuous sense, an update is said to be *numerically conservative* if M at $t = t_{n+1}$ is exactly equal to M at $t = t_n$ minus the fluxes out of the

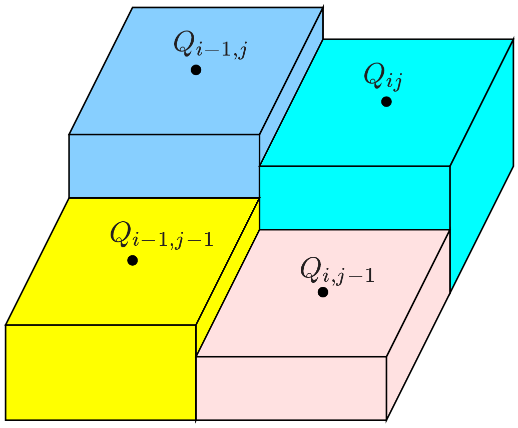

Figure 2.3: Piecewise constant finite volume representation.

boundary of Ω. If we apply the double sum from (2.59) to the finite volume update (2.58), we obtain that

$$\begin{aligned} M^{n+1} = M^n - \Delta t \Delta y \sum_{j=1}^{m_y} \left([\mathcal{F}_1]^{n+1/2}_{m_x+1/2,j} - [\mathcal{F}_1]^{n+1/2}_{-1/2,j} \right) \\ - \Delta t \Delta x \sum_{i=1}^{m_x} \left([\mathcal{F}_2]^{n+1/2}_{i,m_y+1/2} - [\mathcal{F}_2]^{n+1/2}_{i,-1/2} \right) ; \end{aligned} \tag{2.60}$$

and therefore, (2.58) is a numerically conservative update. In particular, if the boundary conditions are set to either *no flux* or *double periodic* (see [53]), then $M^{n+1} = M^n$ exactly. Property (2.60) makes finite volume methods a natural choice for numerically solving conservation laws.

2.4 The $\mathcal{O}(\Delta x^2, \Delta y^2, \Delta t^2)$ wave propagation method

In this section we develop a specific finite volume known as the *wave propagation method.* This method was first introduced in LeVeque [50] for linear advection and in LeVeque [51] for general hyperbolic equations. The method as presented in this text includes the modifications described in [5] for flux functions that are explicit functions of space. The development of this method begins with simple Taylor series arguments.

2.4.1 *The Taylor series expansion*

The Taylor series approximation to $q(x, y, t + \Delta t)$ using information at the point $q(x, y, t)$ can be written as

$$q(x, y, t + \Delta t) = q(x, y, t) + \Delta t\, \partial_t q(x, y, t) + \frac{1}{2} \Delta t^2\, \partial_t^2 q(x, y, t) + \mathcal{O}(\Delta t^3)\,. \tag{2.61}$$

Table 2.1: Type of corrections used in the wave propagation method.

	Type of correction	Terms in series	Effect on update
①	First order upwind	∂_x , ∂_y	$\mathcal{O}(\Delta x, \Delta y, \Delta t)$ update
②	High resolution	∂_x^2 , ∂_y^2	Non-diffusive in smooth regions
③	Transverse	∂_{xy} , ∂_{yx}	Increase stability CFL ≤ 1

We expand $q(x, y, t + \Delta t)$ out to $\mathcal{O}(\Delta t^3)$, because we seek an $\mathcal{O}(\Delta t^2)$ approximation to $\partial_t q(x, y, t)$. If $q(x, y, t)$ satisfies the conservation law (2.51), then the time derivatives in the above Taylor series can all be replaced by derivatives in x and y:

$$\begin{aligned} q(x,y,t+\Delta t) = q - \Delta t &\Big[\underbrace{\partial_x f_1 + \partial_y f_2}_{①}\Big] \\ &+\frac{1}{2}\Delta t^2 \Big[\underbrace{\partial_x \left(A_1 \partial_x f_1\right) + \partial_y \left(A_2 \partial_y f_2\right)}_{②}\Big] \\ &+\frac{1}{2}\Delta t^2 \Big[\underbrace{\partial_y \left(A_2 \partial_x f_1\right) + \partial_x \left(A_1 \partial_y f_2\right)}_{③}\Big] + \mathcal{O}(\Delta t^3)\,, \end{aligned} \tag{2.62}$$

where A_1 and A_2 are the flux Jacobians in the x- and y-directions, respectively. The expansion is divided into a term involving only first derivatives (①), a term involving second derivatives (②), and a term involving cross derivatives (③). The goal of any finite volume method is to generate accurate numerical flux functions $\mathcal{F}_1$ and $\mathcal{F}_2$ in the update (2.58). For the wave propagation method, these numerical flux functions will be constructed from approximations to ①, ②, and ③. The stages in this construction process are the first order upwind corrections (①), the high resolution corrections (②), and the transverse corrections (③). The effect of each correction is summarized in Table 2.1 and developed in detail in the next few sections.

2.4.2 First order upwind corrections

In order for the wave propagation method to be a consistent numerical method, a first order approximation to the terms in ① must be constructed. As was stated in Section 2.3, the solution at time $t = t_n$ is averaged onto the numerical grid using (2.55) in order to produce a piecewise constant representation of $q(x, y, t_n)$ (see Figure 2.3). To first order, the time dynamics of this averaged solution can be computed through a series of 1D Riemann problems across each cell interface. We refer to these as the *normal Riemann problems*. The solutions to the normal Riemann problem are then used in the wave propagation method to construct the numerical fluxes required by a finite volume method.

The wave propagation method as presented in this text utilizes the linearized Riemann solver based on flux differences. At each cell interface $x = x_{i-1/2}$ we are presented with a

Riemann problem of the form

$$\partial_t q + \left[\bar{A}_1\right]_{i-1/2} \partial_x q = 0 \tag{2.63}$$

$$f_1(q,x) = \begin{cases} [f_1]_{i-1} \equiv f_1(Q_{i-1}, x_{i-1}) & \text{if } x < x_{i-1/2} \\ [f_1]_i \equiv f_1(Q_i, x_i) & \text{if } x > x_{i-1/2}\,. \end{cases} \tag{2.64}$$

We require that $\bar{A}_1$ be a *consistent* approximate flux Jacobian (see definition below).

Definition 2.4.1 *An approximate flux Jacobian* $\bar{A}_1$ *is said to be* **consistent** *if for a smooth function* $q(x)$ *the error defined by*

$$E(x,\Delta x) \equiv \partial_q f_1\big(q(x-\Delta x/2), x-\Delta x/2\big) - \bar{A}_1\big(q(x-\Delta x), x-\Delta x, q(x), x\big)$$

satisfies the following two conditions:

1. $E(x,\Delta x) = \mathcal{O}(\Delta x)$ *as* $\Delta x \to 0$. *(*$\Rightarrow \bar{A}_1$ *is first order accurate.)*
2. $E(x,\Delta x) - E(x-\Delta x, \Delta x) = \mathcal{O}(\Delta x^2)$ *as* $\Delta x \to 0$. *(*$\Rightarrow$ *Error is smooth.)*

It can easily be shown that the flux Jacobian based on the arithmetic average in space,

$$\bar{f}_1(q) \equiv \frac{1}{2}\Big([f_1]_i\,(q) + [f_1]_{i-1}\,(q)\Big)\,, \tag{2.65}$$

coupled with either the Roe average or the arithmetic average for q,

$$\bar{Q}_{i-1/2} \equiv \text{Roe average} \tag{2.66}$$

$$\bar{Q}_{i-1/2} \equiv \frac{1}{2}\left(Q_i + Q_{i-1}\right)\,, \tag{2.67}$$

will produce a consistent approximate flux Jacobian. For nonlinear conservation laws we will always use one of these two approximations to the flux Jacobian.

The Riemann solution at cell interface $x = x_{i-1/2}$ to (2.63)-(2.64) can be summarized as follows:

$$\textbf{Flux Difference:}\quad \beta^p_{i-1/2} = l^p_{i-1/2}\cdot\left([f_1]_i - [f_1]_{i-1}\right) \tag{2.68}$$

$$\textbf{Wave Speed:}\quad s^p_{i-1/2} = p^{\text{th}} \text{ eigenvalue of } \left[\bar{A}_1\right]_{i-1/2} \tag{2.69}$$

$$\textbf{Wave Strength:}\quad \mathcal{Z}^p_{i-1/2} = \beta^p_{i-1/2}\, r^p_{i-1/2} \tag{2.70}$$

$$\textbf{Left-going Fluctuation:}\quad \mathcal{A}_1^-\Delta Q_{i-1/2} = \sum_{p:\, s^p_{i-1/2}<0} \mathcal{Z}^p_{i-1/2} + \frac{1}{2}\mathbb{Z}_{i-1/2} \tag{2.71}$$

$$\textbf{Right-going Fluctuation:}\quad \mathcal{A}_1^+\Delta Q_{i-1/2} = \sum_{p:\, s^p_{i-1/2}>0} \mathcal{Z}^p_{i-1/2} + \frac{1}{2}\mathbb{Z}_{i-1/2} \tag{2.72}$$

$$\textbf{Zero speed waves:}\quad \mathbb{Z}_{i-1/2} = \sum_{p:\, s^p_{i-1/2}=0} \mathcal{Z}^p_{i-1/2}\,, \tag{2.73}$$

where $r^p_{i-1/2}$, $s^p_{i-1/2}$, and $l^p_{i-1/2}$ are the p^{th} right eigenvector, eigenvalue, and left eigenvector of $\left[\bar{A}_1\right]_{i-1/2}$, respectively. The left- and right-going fluctuations contain all the wave information propagating to the left and right, respectively. The same procedure is used to solve Riemann problems in the y-direction. We can use the fluctuations to construct a numerical flux of the form

$$[\mathcal{F}_1]_{i-1/2} = \frac{1}{2}\left([f_1]_i + [f_1]_{i-1}\right) + \frac{1}{2}\left(\mathcal{A}_1^+\Delta Q_{i-1/2} - \mathcal{A}_1^-\Delta Q_{i-1/2}\right); \tag{2.74}$$

or equivalently, we can directly use the numerical fluctuations to produce the update

$$\begin{aligned} Q^{n+1}_{ij} = Q^n_{ij} &- \frac{\Delta t}{\Delta x}\left[\mathcal{A}_1^+\Delta Q_{i-1/2,j} + \mathcal{A}_1^-\Delta Q_{i+1/2,j}\right] \\ &- \frac{\Delta t}{\Delta y}\left[\mathcal{A}_2^+\Delta Q_{i,j-1/2} + \mathcal{A}_2^-\Delta Q_{i,j+1/2}\right]. \end{aligned} \tag{2.75}$$

We refer to update (2.75) as the *first order upwind* update, since it is $\mathcal{O}(\Delta x, \Delta y)$ accurate and the solution in any cell is only modified by information propagating into that cell [53]. This update is numerically conservative because

$$\mathcal{A}_1^-\Delta Q_{i-1/2} + \mathcal{A}_1^+\Delta Q_{i-1/2} = \sum_{p=1}^{m} \mathcal{Z}^p_{i-1/2} = [f_1]_i - [f_1]_{i-1}. \tag{2.76}$$

In general, it is necessary to include the zero speed waves ($\mathbb{Z}_{i-1/2}$) in order for us to be able to construct the full flux difference from the left- and right-going fluctuations. This is an artifact of the fact that for a nonlinear Riemann problem we are only using an approximate Riemann solver. In the most general case where $q(x)$ is discontinuous across $x = x_{i-1/2}$, $\mathbb{Z}_{i-1/2} = \mathcal{O}(||Q_i - Q_{i-1}||)$. In Claim 2.4.2 we consider two special cases for which the magnitude of $\mathbb{Z}_{i-1/2}$ is much smaller than $\mathcal{O}(||Q_i - Q_{i-1}||)$.

Claim 2.4.2 *Let* $s^p_{i-1/2} = 0$ *for some* $1 \leq p \leq m$.

(i) *If* $\left[\bar{A}_1\right]_{i-1/2}$ *is constructed from the Roe averages, then* $\mathbb{Z}_{i-1/2} = 0$.

(ii) *If* $\left[\bar{A}_1\right]_{i-1/2}$ *is a consistent flux Jacobian not constructed from the Roe averages and* $q(x)$ *is a smooth function in the region* $\left[x_{i-1/2} - \Delta x/2, x_{i-1/2} + \Delta x/2\right]$ *then*

$$\mathbb{Z}_{i-1/2} \sim \mathcal{O}(\Delta x^2).$$

Proof. Let $\Delta f \equiv [f_1]_i - [f_1]_{i-1}$ and $\Delta Q \equiv Q_i - Q_{i-1}$.

(i) If $\left[\bar{A}_1\right]_{i-1/2}$ is constructed from the Roe averages, then by definition Δf and ΔQ are related through the flux Jacobian:

$$\Delta f = \left[\bar{A}_1\right]_{i-1/2}\Delta Q.$$

We now apply the following manipulations:

$$
\begin{aligned}
& \Delta f = \left[\bar{A}_1\right]_{i-1/2} \Delta Q \\
\Longrightarrow \quad & \Delta f = R_{i-1/2}\, \Lambda_{i-1/2}\, R^{-1}_{i-1/2}\, \Delta Q \\
\Longrightarrow \quad & R^{-1}_{i-1/2}\, \Delta f = \Lambda_{i-1/2}\, R^{-1}_{i-1/2}\, \Delta Q \\
\Longrightarrow \quad & \beta^p_{i-1/2} = s^p_{i-1/2}\, \alpha_{i-1/2}\,.
\end{aligned}
$$

Therefore, if $s^p_{i-1/2} = 0$, then $\beta^p_{i-1/2} = 0$ and

$$
\mathbb{Z}_{i-1/2} = \beta^p_{i-1/2}\, r^p_{i-1/2} = 0\,.
$$

(ii) By Definition 2.4.1, if $q(x)$ is a smooth function then any consistent approximate flux Jacobian $(\left[\bar{A}_1\right]_{i-1/2})$ must approximate the true flux Jacobian to $\mathcal{O}(\Delta x)$. The same must be true of the Roe averaged flux Jacobian $(\left[\bar{A}_{\mathbf{ROE}}\right]_{i-1/2})$. This implies that $\left[\bar{A}_1\right]_{i-1/2}$ and $\left[\bar{A}_{\mathbf{ROE}}\right]_{i-1/2}$ are related as follows:

$$
\left[\bar{A}_{\mathbf{ROE}}\right]_{i-1/2} = \left[\bar{A}_1\right]_{i-1/2} + \Delta x\, M\,,
$$

where M is a matrix with the property that $||M|| \leq k$ and k is a constant independent of Δx. By definition, the Roe averaged flux Jacobian satisfies

$$
\Delta f = \left[\bar{A}_{\mathbf{ROE}}\right]_{i-1/2} \Delta Q = \left[\bar{A}_1\right]_{i-1/2} \Delta Q + \Delta x\, M \Delta Q\,.
$$

If $q(x)$ is smooth, then $||\Delta Q|| = \mathcal{O}(\Delta x)$. We now apply the following manipulations:

$$
\begin{aligned}
& \Delta f = \left[\bar{A}_1\right]_{i-1/2} \Delta Q + \mathcal{O}(\Delta x^2) \\
\Longrightarrow \quad & \Delta f = R_{i-1/2}\, \Lambda_{i-1/2}\, R^{-1}_{i-1/2}\, \Delta Q + \mathcal{O}(\Delta x^2) \\
\Longrightarrow \quad & R^{-1}_{i-1/2}\, \Delta f = \Lambda_{i-1/2}\, R^{-1}_{i-1/2}\, \Delta Q + \mathcal{O}(\Delta x^2) \\
\Longrightarrow \quad & \beta^p_{i-1/2} = s^p_{i-1/2}\, \alpha_{i-1/2} + \mathcal{O}(\Delta x^2)\,.
\end{aligned}
$$

Therefore, if $s^p_{i-1/2} = 0$, then $\beta^p_{i-1/2} = \mathcal{O}(\Delta x^2)$ and

$$
\mathbb{Z}_{i-1/2} = \beta^p_{i-1/2}\, r^p_{i-1/2} = \mathcal{O}(\Delta x^2)\,.
$$

■

2.4.3 An entropy fix for transonic rarefactions

In Section 2.2.5 it was stated that linearizing the Riemann problem can produce an entropy violating solution in the case of a transonic rarefaction. A transonic rarefaction occurs at cell interface $x_{i-1/2}$ if the p^{th} wave is genuinely nonlinear and if

$$\lambda^p_{i-1} < 0 \quad \text{and} \quad \lambda^p_i > 0\,. \tag{2.77}$$

If a transonic rarefaction occurs, we redefine the fluctuations from the linearized Riemann solution at cell $x_{i-1/2}$ to a more diffusive numerical update that is generally less accurate but gives the correct entropy satisfying solution. In particular, we utilize the diffusive local Lax-Friedrichs (LLF) method [53]. For this method the fluctuations needed in update (2.75) are given by

$$\mathcal{A}_1^{\pm}\Delta Q_{i-1/2} = \frac{1}{2}\Big(f_1(Q_i, x_i) - f_1(Q_{i-1}, x_{i-1}) \pm a_{i-1/2}\big(Q_i - Q_{i-1}\big)\Big)\,, \tag{2.78}$$

where

$$a_{i-1/2} \equiv \max\left(\left\| \frac{\partial f_1}{\partial q}(Q_{i-1}, x_{i-1}) \right\|, \left\| \frac{\partial f_1}{\partial q}(Q_i, x_i) \right\| \right)\,. \tag{2.79}$$

At cell interfaces where no transonic rarefactions occur, the fluctuations are computed using (2.71) and (2.72).

2.4.4 High resolution corrections

The next step in developing the full wave propagation method is to consider the terms labeled ② in equation (2.62). We do this by adding correction fluxes to the first order upwind method so that the new update takes the form

$$\begin{aligned} Q^{n+1}_{ij} = Q^n_{ij} &- \frac{\Delta t}{\Delta x}\left(\mathcal{A}_1^{+}\Delta Q_{i-1/2,j} + \mathcal{A}_1^{-}\Delta Q_{i+1/2,j}\right) \\ &- \frac{\Delta t}{\Delta y}\left(\mathcal{A}_2^{+}\Delta Q_{i,j-1/2} + \mathcal{A}_2^{-}\Delta Q_{i,j+1/2}\right) \\ &- \frac{\Delta t}{\Delta x}\left([\tilde{\mathcal{F}}_1]_{i+1/2,j} - [\tilde{\mathcal{F}}_1]_{i-1/2,j}\right) \\ &- \frac{\Delta t}{\Delta y}\left([\tilde{\mathcal{F}}_2]_{i,j+1/2} - [\tilde{\mathcal{F}}_2]_{i,j-1/2}\right)\,. \end{aligned} \tag{2.80}$$

We would like to choose correction fluxes that make both the terms ① and ② accurate to second order. Producing an $\mathcal{O}(\Delta x^2, \Delta y^2)$ approximation to these terms, however, only makes sense if the solution $q(x, y, t)$ remains smooth. Therefore, we would like to construct correction fluxes with the property that in smooth regions they result in an update that approximates ① and ② to second order, but reduce to the first order upwind update in regions where smoothness is lost.

The Lax-Wendroff method produces an update that approximates ① and ② to second order [53]. We can convert the wave propagation method into Lax-Wendroff by defining correction fluxes of the form

$$[\mathcal{F}_1]_{i-1/2} = \frac{1}{2}\sum_p \text{sign}\left(s^p_{i-1/2}\right)\left(1 - \frac{\Delta t}{\Delta x}\left|s^p_{i-1/2}\right|\right)\, \mathcal{Z}^p_{i-1/2}\,. \tag{2.81}$$

Note that it was possible to obtain Lax-Wendroff by only using information already obtained from the Riemann solution. We can introduce a *limited* form of Lax-Wendroff if we define a correction flux of the form

$$[\tilde{\mathcal{F}}_1]_{i-1/2} = \frac{1}{2}\sum_p \mathrm{sign}\left(s^p_{i-1/2}\right)\left(1 - \frac{\Delta t}{\Delta x}|s^p_{i-1/2}|\right)\tilde{\mathcal{Z}}^p_{i-1/2}\,, \tag{2.82}$$

where

$$\tilde{\mathcal{Z}}^p_{i-1/2} \equiv \mathcal{Z}^p_{i-1/2}\,\phi(\theta^p_{i-1/2}). \tag{2.83}$$

In the above expression, ϕ is the *limiter function* and $\theta^p_{i-1/2}$ approximates the magnitude of the solution gradient near $x = x_{i-1/2}$. Since we have already computed a wave decomposition, a natural choice for $\theta^p_{i-1/2}$ is to define it as the the strength of the previous wave compared to the strength of the current wave:

$$\theta^p_{i-1/2} \equiv \frac{\mathcal{Z}^p_{I-1/2}\cdot\mathcal{Z}^p_{i-1/2}}{\mathcal{Z}^p_{i-1/2}\cdot\mathcal{Z}^p_{i-1/2}} \tag{2.84}$$

with

$$I \equiv \begin{cases} i-1 & \text{if} \quad s^p_{i-1/2} > 0 \\ i+1 & \text{if} \quad s^p_{i-1/2} < 0\,. \end{cases} \tag{2.85}$$

The function $\phi(\theta)$ must now be chosen to allow the numerical update to switch between the first order diffusive Godunov update and the second order dispersive Lax-Wendroff method. This flexibility will give the wave propagation method the ability to be accurate in smooth regions and diffusive near discontinuities that would otherwise generate unphysical oscillations.

In order to devise a systemic way for determining how much a given wave needs to be limited, we first define the *total variation* of a one-dimensional grid function Q^n as

$$TV(Q^n) = \sum_{i=-\infty}^{\infty}\left|Q^n_i - Q^n_{i-1}\right|. \tag{2.86}$$

Total variation is thus a measure how much a given grid function Q^n varies over all space.

Definition 2.4.3 *A two-level method is said to be* **total variation diminishing (TVD)** *if, for any set of data Q^n, the values Q^{n+1} computed by the method satisfy $TV(Q^{n+1}) \leq TV(Q^n)$.*

With the aid of a theorem attributed to Harten [35] and further restrictions provided by Sweby [89], it becomes possible to select functions $\phi(\theta)$ that make the wave propagation algorithm total variation diminishing (TVD). A plot of the TVD region provided by Harten's theorem [35] along with the limiter functions needed to construct the second order Lax-Wendroff, Beam-Warming, and Fromm's methods is shown in Figure 2.4(a). Note that all

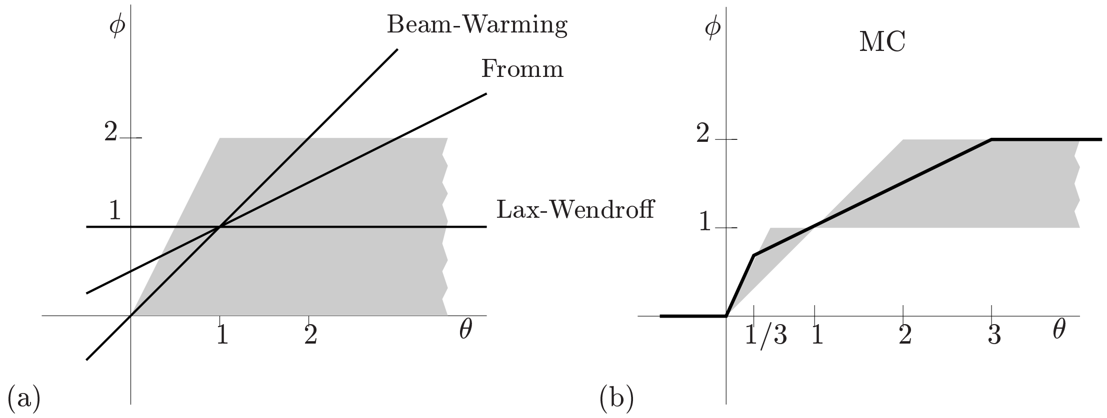

Figure 2.4: (a) Plot of the region in the θ-ϕ plane that guarantees a TVD update. Note that three standard second order methods (Lax-Wendroff, Beam-Warming, and Fromm's method) all exit this region at some value of θ. (b) A plot of the Sweby region and the limiter function for the monotonized centered (MC) limiter. (These plots are courtesy of Randall J. LeVeque [53].)

three methods exit the TVD region at some value of θ. Some common choices for limiter functions that lie in both the TVD and the more restrictive Sweby region are given by

$$\text{minmod:} \quad \phi(\theta) = \begin{cases} 1 & \text{if} \quad |\theta| > 1 \quad \text{and} \quad \theta > 0 \\ \theta & \text{if} \quad |\theta| < 1 \quad \text{and} \quad \theta > 0 \\ 0 & \text{if} \quad \theta \leq 0 \end{cases} \tag{2.87}$$

$$\text{superbee:} \quad \phi(\theta) = \max(0, \min(1, 2\theta), \min(2, \theta)) \tag{2.88}$$

$$\text{van Leer:} \quad \phi(\theta) = \frac{\theta + |\theta|}{1 + |\theta|} \tag{2.89}$$

$$\text{MC:} \quad \phi(\theta) = \max(0, \min((1+\theta)/2, 2, 2\theta))\,. \tag{2.90}$$

In Figure 2.4(b) a plot of the Sweby region along with the MC limiter function is shown. It is important to note that because the update procedure actually depends on the solution through the wave limiter function, the TVD wave propagation method uses a nonlinear numerical update.

2.4.5 Example: 1D advection

We now consider an example in which we compare the Lax-Wendroff scheme and the wave propagation method with the MC limiter. In particular, we consider the advection equation

$$\partial_t q + \partial_x q = 0 \tag{2.91}$$

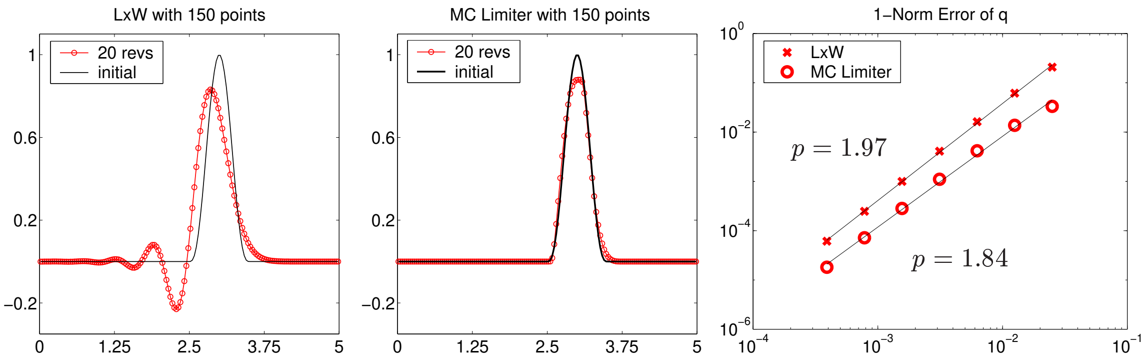

Figure 2.5: A 1D advection equation example. The solution after 20 revolutions is shown using (a) the Lax- Wendroff method and (b) the wave propagation method with the MC limiter. Panel (c) shows that although Lax-Wendroff has a slightly better order of accuracy ($p = 1.97$) than the MC limiter ($p = 1.84$), it is less accurate for all "reasonable grid" resolutions.

with initial and boundary conditions

$$q(x,0) = \begin{cases} P(x) & \text{if } 2.5 < x < 3.5 \\ 0 & \text{otherwise} \end{cases} \tag{2.92}$$

$$\begin{aligned} P(x) \equiv & -64(x-2)^6 + 384(x-2)^5 - 912(x-2)^4 \\ & +1088(x-2)^3 - 684(x-2)^2 + 216(x-2) - 27 \end{aligned} \tag{2.93}$$

$$q(0,t) = q(5,t)\,, \tag{2.94}$$

where the initial condition is chosen so that $q(x,0)$ has at least two continuous derivatives everywhere $\left(q(x,0) \in C^2\right)$. Because (2.91) is linear and constant coefficient, a C^2 initial condition will remain C^2 for all (x,t). The solution using Lax-Wendroff with 150 points is shown in Figure 2.5(a) and using the MC limiter in Figure 2.5(b). The order of accuracy for both of these methods is shown in 2.5(c). As expected, the Lax-Wendroff scheme is second order accurate ($p = 1.97$) and the MC limiter slightly less than second order accurate ($p = 1.84$). What this example shows is that despite the *order* of accuracy, the limiter is considerably more accurate than Lax-Wendroff, especially at coarser resolutions. By limiting waves in regions of large gradients we are able to remove the spurious dispersion generated by a fully second order method. Since the solution is smooth, continuing to increase the resolution (and ignoring round-off errors) will eventually result in the limiters being switched off completely and the two error curves merging.

2.4.6 Transverse corrections

The final term in the Taylor series (2.62) that must be considered for a fully second order method is term ③. Unlike the other two, this term involves cross derivatives; and therefore,

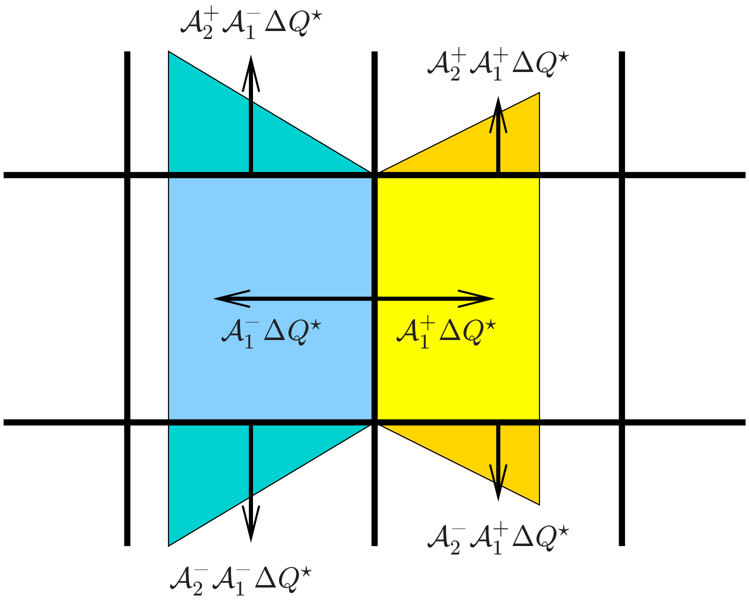

Figure 2.6: Transverse corrections to the wave propagation update are obtained by splitting left- and right-going fluctuations into up- and down-going fluctuations and vice versa.

this term is truly multidimensional in nature. It turns out that term ③ is important not only for improved accuracy, but also for stability properties of the numerical update [53].

The important concept for term ① was the normal Riemann solver and for term ② it was the limiter function. The final concept needed to complete the wave propagation method is the introduction of the *transverse Riemann solver*. In the first order and the high resolution corrections, waves are always assumed to be traveling orthogonal to a cell interface. This is not necessarily true in a multidimensional flow; and therefore, to correct this problem we will introduce another Riemann solver.

The normal Riemann solver produces left- and right-going fluctuations at cell interface $(x_{i-1/2}, y_j)$. Although these fluctuations travel into cell (x_{i-1}, y_j) and (x_i, y_j), cells (x_{i-1}, y_{j-1}), (x_{i-1}, y_{j+1}), (x_i, y_{j-1}), and (x_i, y_{j+1}) should also be modified in a multidimensional problem. To compute how these cells are affected, let us first define left- and right-going fluctuations to which high-resolution corrections have been added:

$$\mathcal{A}_1^\pm \Delta Q^\star_{i-1/2} \equiv \mathcal{A}_1^\pm \Delta Q_{i-1/2} \mp \sum_p \text{sign}\left(s^p_{i-1/2}\right)\left(1 - \frac{\Delta t}{\Delta x}\left|s^p_{i-1/2}\right|\right)\tilde{\mathcal{Z}}^p_{i-1/2}. \tag{2.95}$$

We must now determine how much of each fluctuation travels up and how much travels down. We do this by decomposing the left and right fluctuations using the flux Jacobian in the other coordinate direction:

$$\mathcal{A}_1^\pm \Delta Q^\star_{i-1/2,j} = \mathcal{A}_2^+\mathcal{A}_1^\pm \Delta Q^\star_{i-1/2,j} + \mathcal{A}_2^-\mathcal{A}_1^\pm \Delta Q^\star_{i-1/2,j}. \tag{2.96}$$

Therefore, $\mathcal{A}_2^+\mathcal{A}_1^\pm\Delta Q^\star_{i-1/2,j}$ tells us how much of the left and right fluctuation is up-going and $\mathcal{A}_2^-\mathcal{A}_1^\pm\Delta Q^\star_{i-1/2,j}$ tells us how much is down-going. Since this decomposition again requires us to compute eigenvalues, eigenvectors, and fluctuations, we refer to this decomposition as a *transverse Riemann solution*. An illustration of the multidimensional update process is shown in Figure 2.6.

Once the transverse Riemann problems have been solved, the correction fluxes in update (2.80) are modified in the following way:

$$[\tilde{\mathcal{F}}_2]_{i,j+1/2} = [\tilde{\mathcal{F}}_2]_{i,j+1/2} - \frac{\Delta t}{2\Delta x}\mathcal{A}_2^+\mathcal{A}_1^+\Delta Q^\star_{i-1/2,j} \tag{2.97}$$

$$[\tilde{\mathcal{F}}_2]_{i,j-1/2} = [\tilde{\mathcal{F}}_2]_{i,j-1/2} - \frac{\Delta t}{2\Delta x}\mathcal{A}_2^-\mathcal{A}_1^+\Delta Q^\star_{i-1/2,j} \tag{2.98}$$

$$[\tilde{\mathcal{F}}_2]_{i-1,j+1/2} = [\tilde{\mathcal{F}}_2]_{i-1,j+1/2} - \frac{\Delta t}{2\Delta x}\mathcal{A}_2^+\mathcal{A}_1^-\Delta Q^\star_{i-1/2,j} \tag{2.99}$$

$$[\tilde{\mathcal{F}}_2]_{i-1,j-1/2} = [\tilde{\mathcal{F}}_2]_{i-1,j-1/2} - \frac{\Delta t}{2\Delta x}\mathcal{A}_2^-\mathcal{A}_1^-\Delta Q^\star_{i-1/2,j}\,. \tag{2.100}$$

The same procedure is now carried out to compute how much of the up- and down-going fluctuations travel left and right. After this is done, the correction fluxes $[\tilde{\mathcal{F}}_1]_{i-1/2,j}$ are modified in a completely analogous fashion to $[\tilde{\mathcal{F}}_2]_{i,j+1/2}$ above. This final modification to the correction fluxes provide us with the full wave propagation method in two space dimensions [53].

Claim 2.4.4 *The wave propagation method as described above is an $\mathcal{O}(\Delta x^2, \Delta y^2, \Delta t^2)$ approximation to the exact solution of system of conservation laws*

$$\partial_t q + \partial_x f_1(q,x,y) + \partial_y f_2(q,x,y) = 0 \tag{2.101}$$

in the domain $(x,y,t) \in \Omega$, provided the following conditions are satisfied:

1. *Equation (2.101) is hyperbolic.*
2. *$q(x,y,t) \in C^1$ and $f(q(x,y,t),x,y) \in C^1$ for all $(x,y,t) \in \Omega$.*
3. *$\bar{A}$ is a consistent approximate flux Jacobian.*

Remark. This claim is satisfied if ①, ②, and ③ in (2.62) are approximated to second order. It is shown in [5] that under the above assumptions ① and ② are approximated to second order by the wave propagation method. The same is done for ③ in [53]. ■

Claim 2.4.5 *The wave propagation method as described above is stable for Courant numbers up to 1. The Courant number is defined as*

$$CFL \equiv \max\left(\lambda_1^\star \Delta t/\Delta x, \lambda_2^\star \Delta t/\Delta y\right) \tag{2.102}$$

$$\lambda_1^\star \equiv \max_{p,i,j}\left(|s^p_{i-1/2,j}|\right) \tag{2.103}$$

$$\lambda_2^\star \equiv \max_{p,i,j}\left(|s^p_{i,j-1/2}|\right)\,, \tag{2.104}$$

where $\lambda_1^\star$ and $\lambda_2^\star$ are the maximum wave speeds in the x- and y-directions, respectively.

Remark. Strictly speaking, proofs of Claim 2.4.5 exist only for linear constant coefficient conservation laws. For example, refer to the von Neumann analysis in Section 3.7 of LeVeque [51]. In practice, however, the above claim also works for variable coefficient and nonlinear conservation laws. ■

2.4.7 Example: 2D acoustics

We now consider a multidimensional example in order to demonstrate the accuracy and stability of the wave propagation method. The dynamics of small amplitude sound waves in a background material of density $\rho(x,y)$ and bulk modulus $K(x,y)$ are governed by the conservation law

$$\partial_t \begin{bmatrix} q_1 \\ q_2 \\ q_3 \end{bmatrix} + \partial_x \begin{bmatrix} \rho^{-1} q_2 \\ K q_1 \\ 0 \end{bmatrix} + \partial_y \begin{bmatrix} \rho^{-1} q_3 \\ 0 \\ K q_1 \end{bmatrix} = 0\,, \tag{2.105}$$

where $p = Kq_1$ is the perturbation pressure and $q_2 = \rho u_1$ and $q_3 = \rho u_2$ are the perturbation momentum components [53]. The initial conditions and the background state in this example are taken to be

$$p(x,0) = u_1(x,0) = \begin{cases} 1 & \text{if } -0.35 < x < -0.2 \\ 0 & \text{otherwise} \end{cases} \tag{2.106}$$

$$u_2(x,0) = 0 \tag{2.107}$$

$$\rho(x,y) = 1 \tag{2.108}$$

$$K(x,y) = \frac{1}{\frac{\alpha_{ij}}{0.4} + \frac{1-\alpha_{ij}}{1.0}}\,, \tag{2.109}$$

where α_{ij} is the percentage of grid cell (i,j) which is inside the circle

$$(x - 0.15)^2 + y^2 = 0.25^2\,. \tag{2.110}$$

This creates an initial square pulse that is traveling entirely to the right and a background medium that has a constant density ($\rho = 1$) and a bulk modulus that is discontinuous across the interface defined by (2.110) ($K = 0.4$ inside and $K = 1.0$ outside). The solution to this problem is shown in Figure 2.7. Note that the wave speed is slower inside the circle and that the jump in the bulk modulus causes a reflected wave with a circular shape. This shape is accurately maintained by the multidimensional wave propagation method.

2.5 The nonconservative advection equation

Although they were not considered above, there are some important hyperbolic partial differential equations that cannot be written as conservation laws [53]. The simplest such equation is the advection equation,

$$\partial_t q + u_1 \partial_x q + u_2 \partial_y q = 0\,, \tag{2.111}$$

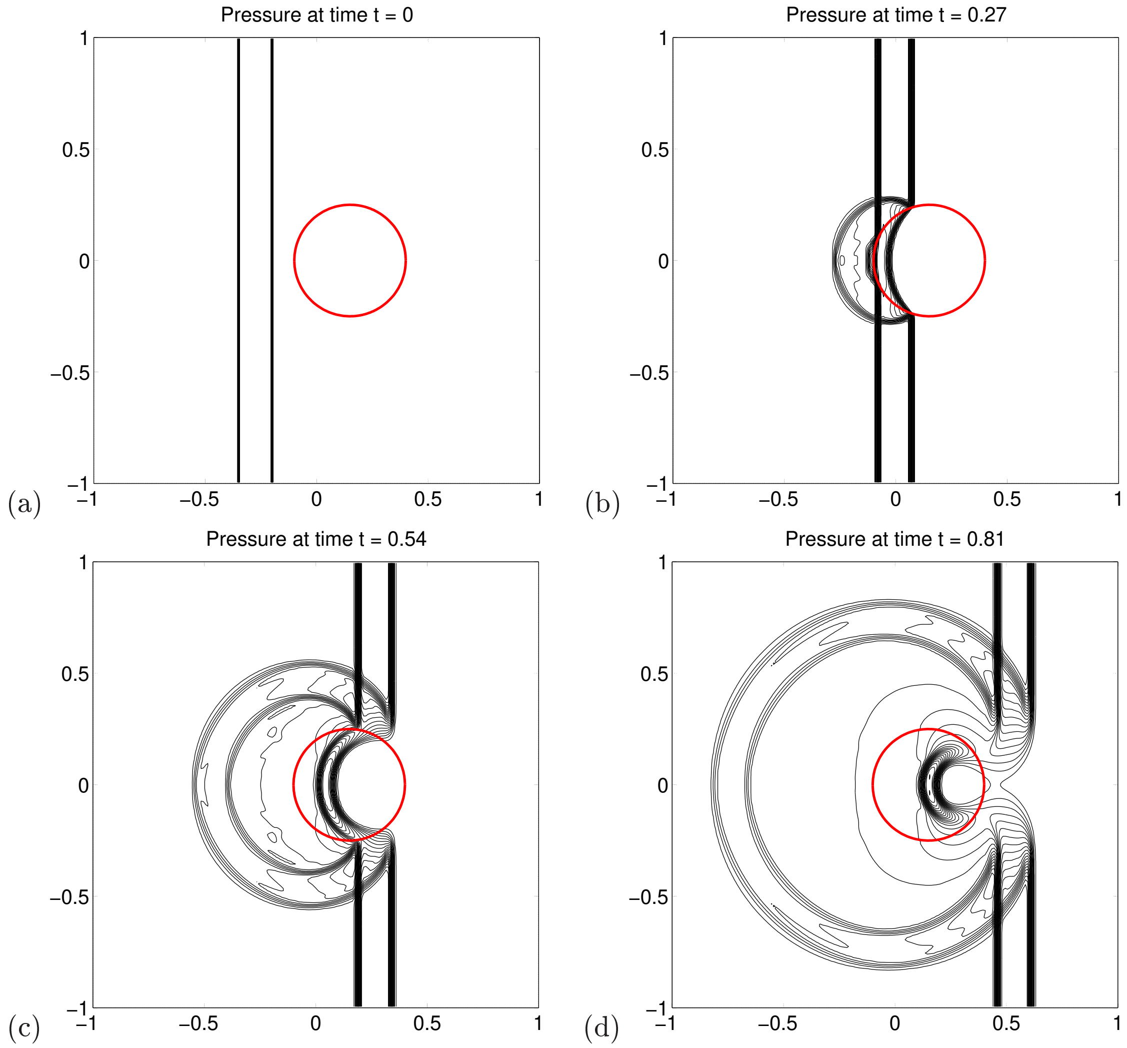

Figure 2.7: A 2D acoustics equation example on a 200×200 Cartesian grid with a Courant number of 0.95. The circular shape of the reflected wave is accurately maintained by the wave propagation method.

which governs the passive transport of a tracer. Here $q = q(x, y, t)$ is the concentration of some tracer and $\mathbf{u} = \mathbf{u}(x, y)$ is the velocity field that determines the local speed and direction of tracer transport. This equation is linear and strictly hyperbolic with eigenvalues u_1 and u_2 in the x- and y-directions, respectively.

In two or more space dimensions the method we advocate in this text is to stagger the concentration and the velocities as shown in Figure 2.8. The wave propagation method can

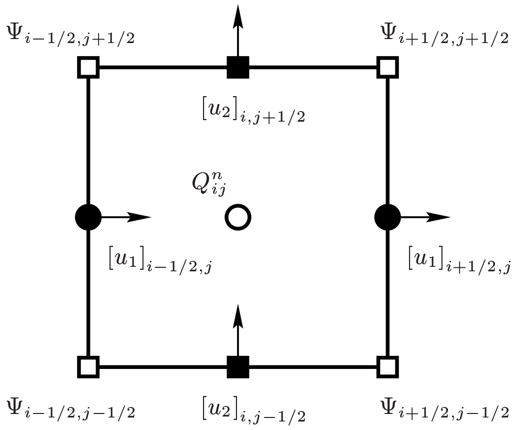

Figure 2.8: Grid staggering for the advection equation.

be used to solve (2.111) if the wave speed and strength are defined as follows:

$$\textbf{Wave Speed:} \quad s^1_{i-1/2} = [u_1]_{i-1/2} \tag{2.112}$$

$$\textbf{Wave Strength:} \quad \mathcal{Z}^p_{i-1/2} = s^1_{i-1/2}\left(Q_i - Q_{i-1}\right). \tag{2.113}$$

No other modifications to the standard method are required.

In the special case of a velocity field that is divergence-free, we advocate introducing a stream function defined by

$$u_1 = \partial_y \Psi \tag{2.114}$$

$$u_2 = -\partial_x \Psi \tag{2.115}$$

and staggering the stream function values as shown in Figure 2.8. If the velocity components at cell edges are computed via

$$[u_1]_{i-1/2,j} = \frac{1}{\Delta y}\left(\Psi_{i-1/2,j+1/2} - \Psi_{i-1/2,j-1/2}\right) \tag{2.116}$$

$$[u_2]_{i,j-1/2} = \frac{1}{\Delta x}\left(\Psi_{i-1/2,j-1/2} - \Psi_{i+1/2,j-1/2}\right), \tag{2.117}$$

then it can be easily verified that

$$[\nabla\cdot\mathbf{u}]_{ij} = \frac{1}{\Delta x}\Big([u_1]_{i+1/2,j} - [u_1]_{i-1/2,j}\Big) + \frac{1}{\Delta y}\Big([u_2]_{i,j+1/2} - [u_2]_{i,j-1/2}\Big) = 0. \tag{2.118}$$

Furthermore, in the case of a divergence-free velocity field the advection equation is exactly equivalent to the conservation law

$$\partial_t q + \partial_x (u_1 q) + \partial_y (u_2 q) = 0. \tag{2.119}$$

It can be shown (see LeVeque [53]) that if the velocities are obtained using (2.116) and (2.117), then the wave propagation method as described above produces a numerically conservative update.

2.6 Conservation laws with a capacity function

In several applications such as ground water flow or flow on non-uniformly spaced grids, the conservation law (2.51) is modified by the introduction of a capacity function:

$$\partial_t (\kappa q) + \partial_x f_1 + \partial_y f_2 = 0\,, \tag{2.120}$$

where $\kappa(x,y) > 0$. The capacity function modifies the *effective size* of a grid cell. In regions where κ is small (large) the effective size of a grid cell is also small (large); and therefore, the magnitude of the fluxes across a grid cell boundary tend to increase (decrease) with a smaller (larger) value of κ. The average amount of q inside the grid cell centered at (x_i, y_j) is now given by

$$Q_{ij}^n \approx \frac{1}{\kappa_{ij}\Delta x \Delta y} \int_{y_{j-1/2}}^{y_{j+1/2}} \int_{x_{i-1/2}}^{x_{i+1/2}} \kappa(\xi,\eta)\, q(\xi,\eta,t_n)\, d\xi\, d\eta \tag{2.121}$$

instead of (2.55). The normal and transverse Riemann problems remain unaltered by the capacity function. The high-resolution correction flux is modified as follows:

$$[\tilde{\mathcal{F}}_1]_{i-1/2} = \frac{1}{2}\sum_p \operatorname{sign}\left(s^p_{i-1/2}\right)\left(1 - \frac{\Delta t}{\kappa_{i-1/2}\Delta x}\left|s^p_{i-1/2}\right|\right) \tilde{\mathcal{Z}}^p_{i-1/2}\,. \tag{2.122}$$

Finally, the numerical update (2.80) must be modified to include the capacity function:

$$\begin{aligned} Q_{ij}^{n+1} = Q_{ij}^n &- \frac{\Delta t}{\kappa_{ij}\Delta x}\left(\mathcal{A}_1^+ \Delta Q_{i-1/2,j} + \mathcal{A}_1^- \Delta Q_{i+1/2,j}\right) \\ &- \frac{\Delta t}{\kappa_{ij}\Delta y}\left(\mathcal{A}_2^+ \Delta Q_{i,j-1/2} + \mathcal{A}_2^- \Delta Q_{i,j+1/2}\right) \\ &- \frac{\Delta t}{\kappa_{ij}\Delta x}\left([\tilde{\mathcal{F}}_1]_{i+1/2,j} - [\tilde{\mathcal{F}}_1]_{i-1/2,j}\right) \\ &- \frac{\Delta t}{\kappa_{ij}\Delta y}\left([\tilde{\mathcal{F}}_2]_{i,j+1/2} - [\tilde{\mathcal{F}}_2]_{i,j-1/2}\right)\,. \end{aligned} \tag{2.123}$$

In this update, the total mass that is conserved is no longer defined by (2.59), but instead by

$$M^n \equiv \Delta x \Delta y \sum_{i=1}^{m_x}\sum_{j=1}^{m_y} \kappa_{ij}\, Q_{ij}^n \approx \int_{x_a}^{x_b}\int_{y_a}^{y_b} \kappa(\xi,\eta)\, q(\xi,\eta,t)\, d\xi\, d\eta\,. \tag{2.124}$$

This new total mass again satisfies relationship (2.60).

The order of accuracy of the method is not affected by the above mentioned modifications to the update. Furthermore, the new update remains stable up to Courant number 1 if in the Courant number (2.102) we redefine maximum wave speeds as follows (see [53]):

$$\lambda_1^\star \equiv \max_{p,i,j}\left(\max\left(-\frac{s^p_{i-1/2,j}}{\kappa_{i-1,j}}, \frac{s^p_{i-1/2,j}}{\kappa_{ij}}\right)\right) \tag{2.125}$$

$$\lambda_2^\star \equiv \max_{p,i,j}\left(\max\left(-\frac{s^p_{i,j-1/2}}{\kappa_{i,j-1}}, \frac{s^p_{i,j-1/2}}{\kappa_{ij}}\right)\right)\,. \tag{2.126}$$

2.7 Balance laws and source terms

The wave propagation method as described thus far is only a method for solving *homogeneous* conservation laws. In many applications, however, the model equations can be written as a conservation law modified by source terms. We refer to these type of equations as *balance laws*. In particular, we consider balance laws of the form

$$\partial_t q + \partial_x f_1(q, x, y) + \partial_y f_2(q, x, y) = \psi(q, x, y, t)\,, \tag{2.127}$$

where ψ is the source term and is a function of q, x, y, and t only. In this section we explore two approaches for extending the wave propagation method to solve balance laws: the Strang splitting approach and the flux modification approach.

2.7.1 Approach 1: Strang splitting

This approach is attributed to G. Strang who popularized this method in a 1968 paper [85]. As the name suggests, the main idea behind this approach is to split an equation into simpler pieces,

$$\partial_t q = \mathcal{L}_1 q + \mathcal{L}_2 q\,, \tag{2.128}$$

and then alternately solving

$$\partial_t q = \mathcal{L}_1 q \tag{2.129}$$

and

$$\partial_t q = \mathcal{L}_2 q \tag{2.130}$$

in such a way as to accurately approximate the solution to the full differential equation (2.128). The natural splitting for balance law (2.127) is to split the conservation and the source term:

$$\mathcal{L}_1 q \equiv -\partial_x f_1(q, x, t) - \partial_y f_2(q, x, t) \tag{2.131}$$

$$\mathcal{L}_2 q \equiv \psi(q, x, t)\,. \tag{2.132}$$

If (2.129) and (2.130) are solved to second order, then to obtain a second order method for the full problem (2.128) one needs to apply the following update (see LeVeque [53]):

$$\textbf{Step 1:}\ \text{(half step with } \mathcal{L}_1) \qquad q^\star = \mathcal{L}_2^{\Delta t/2} q^n \tag{2.133}$$

$$\textbf{Step 2:}\ \text{(full step with } \mathcal{L}_2) \qquad q^{\star\star} = \mathcal{L}_1^{\Delta t} q^\star \tag{2.134}$$

$$\textbf{Step 3:}\ \text{(half step with } \mathcal{L}_1) \qquad q^{n+1} = \mathcal{L}_2^{\Delta t/2} q^{\star\star}\,. \tag{2.135}$$

It should be noted that in general even if (2.129) and (2.130) are solved exactly, there will still be an an $\mathcal{O}(\Delta t^2)$ operator splitting error [53]. The strategy employed in this work is to alternate between a 2-stage Runge-Kutta method for the source term and the wave

Table 2.2: Properties of the Strang splitting approach.

	Properties of the Strang splitting approach
✔	Robust for large class of problems
✘	Spurious oscillations when $\|\|\nabla \cdot F - \psi\|\| \approx 0$
✘	Must have separate BCs for $\partial_t q = \mathcal{L}_1 q$ and $\partial_t q = \mathcal{L}_2 q$

propagation method for the homogeneous conservation law:

$$\textbf{Step 1:}\ \mathcal{L}_2^{\Delta t/2} \equiv \begin{cases} Q_{ij}^{\diamondsuit} = Q_{ij}^n + \frac{\Delta t}{4}\,\psi\left(Q_{ij}^n, x_i, y_j, t\right) \\ Q_{ij}^{\star} = Q_{ij}^n + \frac{\Delta t}{2}\,\psi\left(Q_{ij}^{\diamondsuit}, x_i, y_j, t+\frac{\Delta t}{4}\right) \end{cases} \tag{2.136}$$

$$\textbf{Step 2:}\ \mathcal{L}_1^{\Delta t} \equiv \text{The wave propagation method } \left(Q^{\star} \longrightarrow Q^{\star\star}\right) \tag{2.137}$$

$$\textbf{Step 3:}\ \mathcal{L}_2^{\Delta t/2} \equiv \begin{cases} Q_{ij}^{\diamondsuit} = Q_{ij}^{\star\star} + \frac{\Delta t}{4}\,\psi\left(Q_{ij}^{\star\star}, x_i, y_j, t+\frac{\Delta t}{2}\right) \\ Q_{ij}^{n+1} = Q_{ij}^{\star\star} + \frac{\Delta t}{2}\,\psi\left(Q_{ij}^{\diamondsuit}, x_i, y_j, t+\frac{3\Delta t}{4}\right) \end{cases} . \tag{2.138}$$

The advantage of Strang splitting is that it works well for a wide range of problems. The main disadvantage is that spurious oscillations are generated in flow regimes where there is a steady or quasi-steady state: $||\nabla \cdot F - \psi|| \approx 0$. The oscillations occur because the two pieces of the equation that should be in balance, the divergence of the flux tensor and the source term, are split into separate operators. The $\mathcal{O}(\Delta t^2)$ error that is made because of the Strang splitting means that at best $||\nabla \cdot F - \psi|| = \mathcal{O}(\Delta t^2)$. If in the exact solution $||\nabla \cdot F - \psi|| \ll \mathcal{O}(\Delta t^2)$, then Strang splitting produces an approximation with a large relative error (i.e., the spurious oscillations). Another possible disadvantage with Strang Splitting is that boundary conditions must be specified on the two subproblems (2.129) and (2.130). In some applications, these conditions may be more difficult to obtain than the boundary conditions for the full equation (2.128). The above comments are summarized in Table 2.2.

2.7.2 Approach 2: Modifying the flux differences

In order to overcome the problems experienced by the Strang splitting approach, several alternative methods have been introduced in the literature. In particular, those methods most compatible with the wave propagation method are the quasi-steady method introduced in LeVeque [52], the Rankine-Hugoniot-Riemann solver of Jenny and Müller [43], and the flux difference method of LeVeque and Pelanti [58].

In LeVeque [52] and LeVeque and Bale [55], an approach called the *quasi-steady* method is developed and applied to the shallow water and Euler equations, respectively. For strictly quasi-steady flows this method produces very accurate results. The method is based on introducing an additional Riemann problem at cell centers which requires that in each grid cell a nonlinear algebraic equation be solved. In general, this nonlinear solution process makes the overall method more expensive; and furthermore, the algebraic equation can fail to have a solution if the flow is far from a steady-state.

A similar method called the *Rankine-Hugoniot-Riemann* solver is derived in Jenny and Müller [43]. Instead of introducing a new Riemann problem at cell centers, this method modifies the Riemann problem at the cell edges. This method still requires the solution to a nonlinear algebraic equation, but seems to work better for flows further away from steady state than the quasi-steady method.

In LeVeque and Pelanti [58], a new approximate Riemann solver is developed that is based on flux differences. Furthermore, they discuss a modification of this Riemann solver capable of solving balance laws with source terms. It is similar to the approach of Jenny and Müller [43] in the sense that the Riemann problems are modified only at cell edges, but this method does not require the solution to a nonlinear algebraic equation. In [5] a second order correction is added to this method and the method is successfully applied to a linearized shallow water flow. In the remainder of this section we describe a 2D extension of this method.

As was discussed in previous sections, the wave propagation method is based on solving a series of one-dimensional Riemann problems at cell edges. This fact prompts us to divide the source term into two separate pieces,

$$\psi = \psi_1 + \psi_2 \, , \tag{2.139}$$

such that $\psi_1 = 0$ if $\partial_x q \equiv 0$ and $\psi_2 = 0$ when $\partial_y q \equiv 0$. The normal Riemann problems that must be solved in the x- and y-directions are now based on the equations

$$\partial_t q + \partial_x f_1 = \psi_1 \tag{2.140}$$
$$\partial_t q + \partial_y f_2 = \psi_2 \, , \tag{2.141}$$

respectively. The goal is to develop Riemann solvers for equations (2.140) and (2.141) that directly incorporate the corresponding source term and that produce accurate solutions in flow regimes where

$$\partial_x f_1 \approx \psi_1 \tag{2.142}$$
$$\partial_y f_2 \approx \psi_2 \, . \tag{2.143}$$

Numerically, (2.142) and (2.143) can be written as

$$[f_1]_{ij} - [f_1]_{i-1,j} \approx \Delta x \, [\psi_1]_{i-1/2,j} \tag{2.144}$$
$$[f_2]_{ij} - [f_2]_{i,j-1} \approx \Delta y \, [\psi_2]_{i,j-/1/2} \, . \tag{2.145}$$

We recall that the Riemann solvers described in previous sections were based on decomposing flux differences; and furthermore, we note that the above expressions can be written as a modified flux difference:

$$\Delta f_1 \equiv [f_1]_{ij} - [f_1]_{i-1,j} - \Delta x \, [\bar{\psi}_1]_{i-1/2,j} \tag{2.146}$$
$$\Delta f_2 \equiv [f_2]_{ij} - [f_2]_{i,j-1} - \Delta y \, [\bar{\psi}_2]_{i,j-1/2} \, , \tag{2.147}$$

where the source term at the cell edge can be approximated via simple averaging:

$$[\bar{\psi}_1]_{i-1/2,j} \approx \frac{1}{2} \left([\psi_1]_{ij} + [\psi_1]_{i-1,j} \right) . \tag{2.148}$$

The new Riemann solver for solving balance law (2.127) is therefore nothing more than the old Riemann solver for solving conservation law (2.51) with a modified flux difference input. For flows near a steady state, Δf_1 and Δf_2 will be close to zero; and therefore, the approximate Riemann solver will generate only very small amplitude waves.

We must now verify that with the above modifications to the flux differences, we can obtain an $\mathcal{O}(\Delta x^2, \Delta y^2, \Delta t^2)$ approximation to the solution of balance law (2.127). The semi-discrete Taylor series approximation to (2.127) is given by

$$
\begin{aligned}
q(x,y,t+\Delta t) = q - \Delta t &\Big[\underbrace{(\partial_x f_1 - \psi_1) + (\partial_y f_2 - \psi_2)}_{①}\Big] \\
+\frac{1}{2}\Delta t^2 &\Big[\underbrace{\partial_x \{A_1 (\partial_x f_1 - \psi_1)\} + \partial_y \{A_2 (\partial_y f_2 - \psi_2)\}}_{②}\Big] \\
+\frac{1}{2}\Delta t^2 &\Big[\underbrace{\partial_y \{A_2 (\partial_x f_1 - \psi_1)\} + \partial_x \{A_1 (\partial_y f_2 - \psi_2)\}}_{③}\Big] \\
+\frac{1}{2}\Delta t^2 &\underbrace{\left[\left.\frac{\partial \psi}{\partial t}\right|_q + \partial_q \psi \cdot \Big\{(\partial_x f - \psi_1) + (\partial_y f - \psi_2)\Big\}\right]}_{④} + \mathcal{O}(\Delta t^3),
\end{aligned}
\tag{2.149}
$$

where the term $(\partial\psi/\partial t)|_q$ denotes the time derivative of $\psi(q(x,t),x,y,t)$ keeping $q(x,t)$ constant. The terms labeled ①, ②, and ③ are approximated to $\mathcal{O}(\Delta x^2, \Delta y^2)$ through the use of the previously described upwind corrections, high resolution corrections, and transverse corrections, respectively, if the modified flux differences (2.146) and (2.147) are used in place of the standard flux differences. Bale et al. [5] show that an $\mathcal{O}(\Delta x^2, \Delta y^2)$ approximation to the term labeled ④ can be constructed from the wave information already provided by the normal Riemann solver:

$$
\begin{aligned}
Q_{ij}^{n+1} = Q_{ij}^n + \ldots + \frac{1}{2}\Delta t^2 &\left[\left.\frac{\partial \psi}{\partial t}\right|_q\right]_{ij} \\
- \frac{\Delta t^2}{2\Delta x} [\partial_q \psi]_{ij} \cdot &\left[\sum_{p=1}^{m} \frac{1}{2}\big(\mathcal{Z}_{i-1/2}^p + \mathcal{Z}_{i+1/2}^p\big) + \sum_{p=1}^{m} \frac{1}{2}\big(\mathcal{Z}_{j-1/2}^p + \mathcal{Z}_{j+1/2}^p\big)\right],
\end{aligned}
\tag{2.150}
$$

where $\mathcal{Z}_{i-1/2}^p$ and $\mathcal{Z}_{j-1/2}^p$ are the waves generated by normal Riemann solvers in the x- and y-directions, respectively. With correction (2.150) the flux modification approach is fully $\mathcal{O}(\Delta x^2, \Delta y^2)$ for smooth problems, the same order of accuracy as that of the Strang splitting approach.

The advantage of the flux modification approach over Strang splitting is that for flow regimes near a steady state of the form (2.142)-(2.143), no spurious oscillations are introduced. Furthermore, boundary conditions are imposed on the full equation (2.127) rather than on subproblems. The advantage over the quasi-steady approach is that no nonlinear algebraic equation must be solved, allowing the flux modification approach to also work

Table 2.3: Properties of the flux modification approach.

	Properties of the approach based on modifying the flux differences
✔	Accurate when $\partial_x f_1 \approx \psi_1$ and $\partial_y f_2 \approx \psi_2$
✔	Can also handle flows not near steady state
✔	BCs applied on a single equation
✘	Spurious oscillations for complicated steady states (i.e., $\partial_x f_1 + \partial_y f_2 \approx \psi$)
✘	Strang splitting is more accurate when it is not clear how to split $\psi = \psi_1 + \psi_2$

well for flow regimes further away from steady state. On the other hand, the disadvantage of this scheme is that it produces much of the same spurious oscillations present in Strang splitting when the solution is near a more complicated steady state than (2.142)-(2.143). For example, if the steady state is a multidimensional balance of flux and source,

$$\partial_x f_1 + \partial_y f_2 = \psi \,, \tag{2.151}$$

the flux modification may also produce spurious oscillations. Furthermore, for some source terms it may not always be clear how to separate the source term into $\psi = \psi_1 + \psi_2$. When this separation is not obvious, Strang splitting is often more accurate than the flux modification approach. The above comments are summarized in Table 2.3. In the remainder of this work we utilize the flux modification approach whenever an obvious separation $\psi = \psi_1 + \psi_2$ exists and the Strang splitting approach otherwise.

2.7.3 Example: Rayleigh-Taylor instability

In order to see the benefits of the flux modification approach for handling source terms, we consider a Rayleigh-Taylor instability example taken from LeVeque and Bale [55] for the two-dimensional Euler equations,

$$\partial_t \begin{bmatrix} \rho \\ \rho u_1 \\ \rho u_2 \\ \mathcal{E} \end{bmatrix} + \partial_x \begin{bmatrix} \rho u_1 \\ \rho u_1^2 + p \\ \rho u_1 u_2 \\ u_1(\mathcal{E}+p) \end{bmatrix} + \partial_y \begin{bmatrix} \rho u_2 \\ \rho u_1 u_2 \\ \rho u_2^2 + p \\ u_2(\mathcal{E}+p) \end{bmatrix} = \begin{bmatrix} 0 \\ \rho\, \partial_x \phi \\ \rho\, \partial_y \phi \\ 0 \end{bmatrix} . \tag{2.152}$$

The pressure is related to the other unknowns through the equation of state

$$\mathcal{E} = \frac{p}{\gamma - 1} + \frac{1}{2}\rho |\mathbf{u}|^2 + \rho\phi. \tag{2.153}$$

In the above equations, the unknowns are the density ρ, the velocity $\mathbf{u}$, the pressure p, and the energy $\mathcal{E}$. $\phi(x, y)$ is the gravitational potential and γ is the gas constant for a polytropic gas. The components of this equation are the conservation of mass, the conservation of momentum, the conservation of energy. In this problem it is natural to split the source term into the following pieces:

$$\psi_1 \equiv \begin{bmatrix} 0 \\ \rho\,\partial_x\phi \\ 0 \\ 0 \end{bmatrix} \qquad \psi_2 \equiv \begin{bmatrix} 0 \\ 0 \\ \rho\,\partial_y\phi \\ 0 \end{bmatrix} . \tag{2.154}$$

The discretization of this source term at cell interfaces is taken as

$$\left[\bar{\psi}_1\right]_{i-1/2} \equiv \begin{bmatrix} 0 \\ \frac{1}{2}\left(\rho_i + \rho_{i-1}\right)\phi_{i-1/2} \\ 0 \\ 0 \end{bmatrix} \quad \left[\bar{\psi}_2\right]_{j-1/2} \equiv \begin{bmatrix} 0 \\ 0 \\ \frac{1}{2}\left(\rho_j + \rho_{j-1}\right)\phi_{j-1/2} \\ 0 \end{bmatrix} . \tag{2.155}$$

We consider an initial condition comprised of two gases with the same gas constant ($\gamma = 1.4$) but different temperatures separated by an interface. Each gas is in isothermal equilibrium under the gravitational potential $\phi(r,\theta) = -r$, where r and θ are the standard polar coordinates. Specifically, $u_1 = u_2 = 0$ and the density and pressure are given by

$$\rho(r,\theta,0) = \begin{cases} \rho_1(r) & \text{if} \quad 0 < r < \bar{r}(\theta) \\ \rho_2(r) & \text{if} \quad \bar{r}(\theta) < r \end{cases} \tag{2.156}$$

$$p(r,\theta,0) = \begin{cases} \frac{3}{5\log(5)}\,\rho_1(r) & \text{if} \quad 0 < r < \bar{r}(\theta) \\ \frac{3}{10\log(5)}\,\rho_2(r) & \text{if} \quad \bar{r}(\theta) < r\,, \end{cases} \tag{2.157}$$

where

$$\rho_1(r) \equiv \frac{1}{2}\,e^{-\left(\frac{5}{3}\log(5)\right)\,r} \tag{2.158}$$

$$\rho_2(r) \equiv 5\,e^{-\left(\frac{10}{3}\log(5)\right)\,r} \tag{2.159}$$

$$\bar{r}(\theta) \equiv \frac{3}{5}\left(1 + \epsilon\cos(20\,\theta)\right) . \tag{2.160}$$

Although the two gases are unstably stratified (i.e., the lighter gas is *underneath* the heavier gas), with $\epsilon = 0$ the initial conditions are an exact steady state solution to the Euler equations. For a small perturbation ($0 < \epsilon \ll 1$) of the interface separating the two gases, however, the initial condition will become unstable and the gases will try to obtain a stably stratified state (i.e., the lighter gas moves up and the heavier gas down). Taking $\epsilon = 0.02$ produces the initial condition shown in the top right panel of Figure 2.9. Through symmetry we can restrict ourselves to the domain $(x,y) \in [0,1] \times [0,1]$ with non-reflecting boundary conditions at the top ($y = 1$) and the right ($x = 1$) and solid wall boundary conditions at the bottom ($y = 0$) and the left ($x = 0$). The solutions at $t = 0$, $t = 0.8$, $t = 1.4$, and $t = 2$ on a grid with 100×100 points are shown in panel form in Figure 2.9. The solution presented here compares well to the one computed by the quasi-steady solver in LeVeque and Bale [55]. Unlike the quasi-steady solver, however, the current method requires neither the solution to a nonlinear algebraic system nor the use of Strang splitting when the flow because sufficiently unsteady. Because the initial conditions are so close to an exact steady

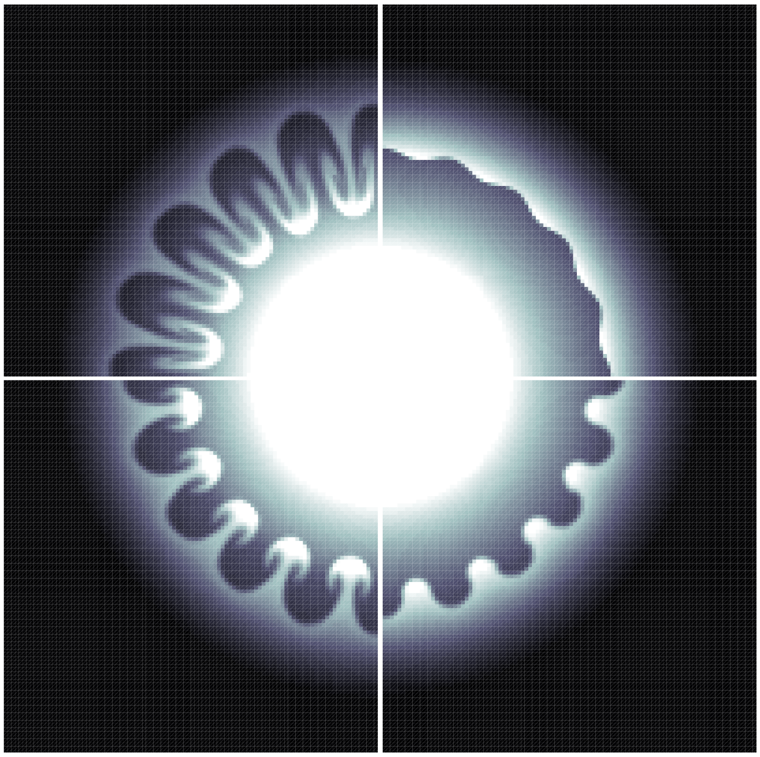

Figure 2.9: Rayleigh-Taylor instability with an inward pointing gravitational field. The four panels display the density on a 100×100 Cartesian grid at time $t = 0$ (upper right), $t = 0.8$ (lower right), $t = 1.4$ (lower left), and $t = 2$ (upper left). The numerical discretization captures both the dynamics at the initial quasi-steady state and the fully unsteady flow that develops soon after.

state, the use of Strang splitting at the same resolution as above produces a very inaccurate solution [55].

A slight modification of the code that was used for the above example is used in Anitei and Breidenthal [1]. In this paper the authors consider several Rayleigh-Taylor problems with various downward pointing gravitational forces (i.e., $\phi(x, y) = -y$). In all of their examples they begin with an initial condition that is a slight perturbation of a steady sate.

2.8 The CLAWPACK *software*

The wave propagation method as described above has been implemented in the CLAWPACK software package [49]. Throughout this work will make use of CLAWPACK as a tool to implement the numerical methods which we develop. In later chapters we will also make use of the CLAWMAN software package [2]. This package is developed in [3, 4, 6] and provides a variant of CLAWPACK specifically designed for solving conservations on curved manifolds. Both CLAWMAN and CLAWPACK are freely available. Although not directly used in this work, the adaptive mesh refinement version of the wave propagation method as described in Berger and LeVeque [10] is also freely available in the AMRCLAW software package [56]. The three dimensional extension of the wave propagation method given in Langseth and LeVeque [46] has also been built into the CLAWPACK and AMRCLAW packages. Recently, a parallel and adaptive mesh refinement version of CLAWPACK that contains various additional features has been developed by S. Mitran. This software is called BEARCLAW and is also freely available [57, 66].